AIP | Applied Physics Letters

Structural study of Bi2Sr2CaCu2O8+δ exfoliated nanocrystals

A. Lupascu, Renfei Feng, L. J. Sandilands, Zixin Nie, V. Baydina et al.

Citation: Appl. Phys. Lett. **101**, 223106 (2012); doi: 10.1063/1.4768234
View online: http://dx.doi.org/10.1063/1.4768234
View Table of Contents: http://apl.aip.org/resource/1/APPLAB/v101/i22
Published by the American Institute of Physics.

Structural study of $Bi_2Sr_2CaCu_2O_{8+\delta}$ exfoliated nanocrystals

A. Lupascu,[1] Renfei Feng,[2] L. J. Sandilands,[1] Zixin Nie,[1] V. Baydina,[1] Genda Gu,[3] Shimpei Ono,[4] Yoichi Ando,[5] D. C. Kwok,[6] N. Lee,[6] S.-W. Cheong,[6] K. S. Burch,[1] and Young-June Kim[1,a)]

[1]*Department of Physics, University of Toronto, 60 St. George Street, Toronto, Ontario M5S 1A7, Canada*
[2]*Canadian Light Source, 101 Perimeter Road, Saskatoon, Saskatchewan S7N 0X4, Canada*
[3]*Department of Condensed Matter Physics and Materials Science, Brookhaven National Laboratory, Upton, New York 11973-5000, USA*
[4]*Central Research Institute of Electric Power Industry, Yokosuka, Kanawaga 240-0196, Japan*
[5]*Institute of Scientific and Industrial Research, Osaka University, Ibaraki, Osaka 567-0047, Japan*
[6]*Department of Physics and Astronomy, Rutgers Center for Emergent Materials, Rutgers University, 136 Frelinghuysen Road, Piscataway, New Jersey 08854, USA*

(Received 18 October 2012; accepted 3 November 2012; published online 26 November 2012)

We demonstrate that structural and spectroscopic information can be obtained on exfoliated nanocrystals as thin as 6 nm. This can be achieved by using a combination of micro X-ray fluorescence (μXRF), micro X-ray absorption near-edge spectroscopy (μXANES), and X-ray microdiffraction (μXRD) techniques. Highly focused, tunable X-ray beams available at synchrotron sources enable one to use these non-invasive characterization tools to study exfoliated samples on a variety of substrates. As an example, we focused on exfoliated nanocrystals of the high temperature superconductor $Bi_2Sr_2CaCu_2O_{8+\delta}$. μXRF is used to locate the sample of desired thickness; μXANES and μXRD are used to obtain electronic and structural information, respectively. We find that the "4.7b" structural modulation, characteristic of the bulk crystals, is drastically suppressed for exfoliated crystals thinner than 60 nm. © *2012 American Institute of Physics*.
[http://dx.doi.org/10.1063/1.4768234]

Mechanical exfoliation, first used to create graphene,[1] has become a promising method for producing a variety of low-dimensional materials: MoS_2, $NbSe_2$, $Bi_2Sr_2CaCu_2O_{8+\delta}$ (Bi-2212),[1,2] BN,[3] Bi_2Se_3,[4] and Bi_2Te_3.[5,6] Compared to deposited films, where chemical bonds are formed between the substrate and the film, exfoliated nanocrystals are made by pressing a bulk crystal, which was grown slowly through a nucleation process, and held on the substrate by friction.[1,2] Being the thinner replica of the bulk material, exfoliated nanocrystals are expected to have a crystal structure identical to the bulk and smaller influence from the substrate materials, unlike deposited films. Given the increased interest in exfoliated nanocrystals, structural studies are needed for assessing their crystalline quality and detecting degradation caused by chemical processing and exposure to air. In addition, structural studies can shed light on how materials properties change as the system becomes quasi two-dimensional. Recently, changes in band structures[7,8] and Raman spectra[3,4,9,10] have been observed as the thickness of exfoliated nanocrystals decreases.

Direct structural studies of exfoliated nanocrystals, however, are quite difficult. Transmission electron microscopy (TEM), commonly used for structural characterization, has been used to study nanocrystals.[1,6,9,10] The TEM sample preparation is restricted to a limited selection of substrates, namely SiN or carbon/copper grids, and is often accompanied by exposure to chemicals and strain.[9] Unlike TEM, X-ray techniques allow a variety of substrates, enabling the study of subtle substrate influence on the exfoliation method. However, conventional X-ray diffraction is challenged by the small lateral size of the exfoliated samples (typically tens of microns or smaller).

The size challenge for conventional X-rays can be overcome by using a synchrotron X-ray beam, focused to micron-sized beam with Kirkpatrick-Baez (KB) mirror-optics.[11–13] These mirrors maintain the energy tunability of the beam, enabling both spectroscopic [micro X-ray fluorescence (μXRF), micro X-ray absorption near-edge spectroscopy (μXANES)] and structural [X-ray microdiffraction (μXRD)] studies. This non-invasive method requires no additional sample preparation or chemical treatment and can be used to study samples on various substrates. Using these techniques, we performed structural studies on $Bi_2Sr_2CaCu_2O_{8+\delta}$ nanocrystals exfoliated on a Si/SiO_2 substrate.[14] The synchrotron studies were carried out at the VESPERS Beamline of the Canadian Light Source. A diagram of the experimental setup is shown in Fig. 1(a). VESPERS is a bending magnet beamline with KB mirror optics, with an effective beam spot of approximately (3×3) μm over a wide energy range.[15] The beamline allows the use of a polychromatic beam as well as three different choices for monochromators. A quasi-monochromatic beam (bandwidth of $\sim$1.6 %), produced with a multilayer monochromator in the energy range of 15–17 keV, was used for μXRD. Note that at this energy, the X-ray attenuation due to the Si/SiO_2 substrate is approximately 50%, and we could obtain a diffraction pattern in transmission mode, using a Mar165 CCD detector. The sample-detector distance was calibrated with LaB_6 powder, and the FIT2D software was used for analysis.[16]

The accurate positioning of the X-ray beam on the sample, a critical step in the experiment, is achieved via micro X-ray fluorescence mapping. A polychromatic beam with

a)Electronic mail: yjkim@physics.utoronto.ca.

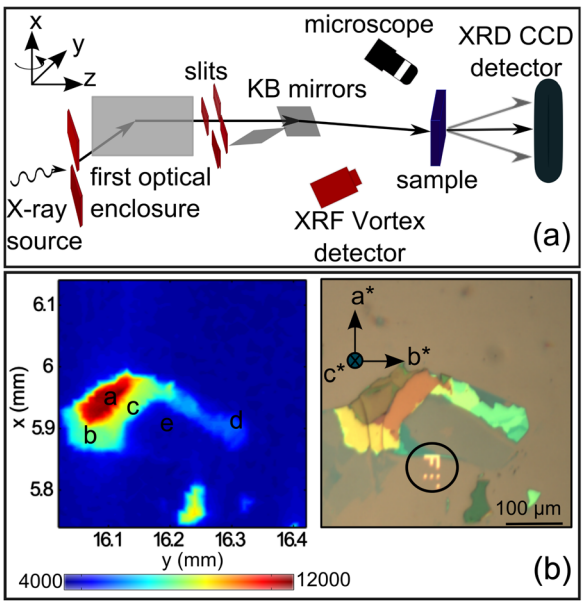

FIG. 1. (a) Experimental setup: The μXRD experiment was performed in transmission mode, using a CCD detector. The accurate positioning of the beam on the sample was done via μXRF mapping with a Vortex detector. The energy for diffraction was fixed with a double multilayer monochromator (~1.6 % bandpass), located in the first optical enclosure. A pair of KB mirrors is used to steer and focus the beam (see Ref. 15 for a detailed description of the VESPERS beamline). (b) The Cu Kα line fluorescence map of a Bi-2212 exfoliated nanocrystal (left), and the corresponding optical microscope image (right). The thickness range is a > 250 nm, b = 69 nm, c = 45 nm, d = 40 nm, and e = 10 nm. The crystallographic axes of the sample are a*—corresponds to the x-axis, b*—corresponds to the y-axis, and c*—corresponds to the z-axis.

an energy range of 6–30 keV was used to scan the samples and produce element-specific μXRF maps. Several emission lines were selected to scan the nanocrystals: Au Lα, Bi Lα, Bi Lβ, Sr Kα, Cu Kα, and Ca Kα. The μXRF spectrum was collected with a Vortex silicon drift detector, by scanning the sample in the x-y plane (see Fig. 1(b) for coordinates). First, the gold markers deposited on the substrate were identified via the Au Lα emission line. Subsequently, the beam was moved in a region of interest by using the gold markers as guides, and a μXRF map of an exfoliated sample was acquired and compared to the optical image. A Cu Kα line μXRF map and the corresponding optical image of a Bi-2212 nanocrystal are presented in Fig. 1(b). Since the map is element specific, the gold marker indicated with a black circle in the optical image is not present in the fluorescence map for the Cu Kα line. The μXRF intensity pattern corresponds to the sample thickness distribution. A comparison of the μXRF maps to the optical microscope images allowed the identification of the samples. The μXRF maps obtained for the emission lines of the other Bi-2212 constituent elements look very similar. The fluorescence intensity (I) as a function of thickness (t) obeys a linear relation: $I \propto t$, which is expected in the very thin nanocrystal limit.[14] The μXRF data can thus be used as an independent in-situ method for confirming the thickness of the exfoliated crystals.

X-ray absorption spectroscopy probes unoccupied band structure through core electron transitions. The oxidation state of an element and its coordination environment can be studied with μXANES. The high sensitivity of this technique enables measurements on very small sample volumes even with a high background, making it suitable for exploring the electronic properties of nanocrystals. μXANES data were acquired using a monochromatic beam produced by a Si (111) monochromator ($E/\Delta E \sim 10\,000$) and the same Vortex detector used for μXRF mapping. The data were collected at the Cu K-edge for optimally doped (OP) and underdoped (UD) Bi-2212, with the X-ray beam polarized in the Cu-O plane. Fig. 2 shows the normalized Cu K-edge μXANES spectra for OP Bi-2212 exfoliated samples of 205 nm, 69 nm, and 6 nm. The μXANES spectra are compared to reference data of Bi-2212 bulk single crystal.[17] The intense peak around 8990 eV and all higher energy features of the bulk crystal are reproduced in the exfoliated nanocrystals. The features of the nanocrystals seem sharper, since the experiment was carried out in transmission, avoiding the self-absorption effect. No significant difference was observed between OP and UD samples. Fig. 2 (inset) contains the μXANES intensity of the exfoliated samples normalized by their thickness, indicating that the intensity is proportional to the sample thickness. The reduced thickness does not seem to affect the electronic properties of the nanocrystals, in particular the Cu-valence. The local electronic structure remains identical throughout the entire thickness range, confirming the integrity of the crystal.

Two methods were used for microdiffraction: angle-integration and wavelength-integration. For the angle-integration, the sample was rotated by ~5° around the x-axis in steps of ~0.3° using a piezo-motor. The diffraction images acquired after every rotation were summed up, resulting in an angle-integrated diffraction image. For the wavelength-integration, diffraction images were captured over an energy range of 15–17 keV in steps of 250 eV (wavelength steps of ~0.01 Å). The raw images were adjusted for the wavelength shift before being integrated over the entire wavelength range, yielding the wavelength-integration image.

In Fig. 3, we present the angle integrated diffraction patterns from OP Bi-2212 exfoliated crystals of (a) 69 nm and (b) 12 nm. The rectangular block in the middle and the faint horizontal strip on the right of the diffraction patterns in Fig. 3 are shadows from the beam-stop and its post. The experimental geometry was chosen so that the Bragg condition

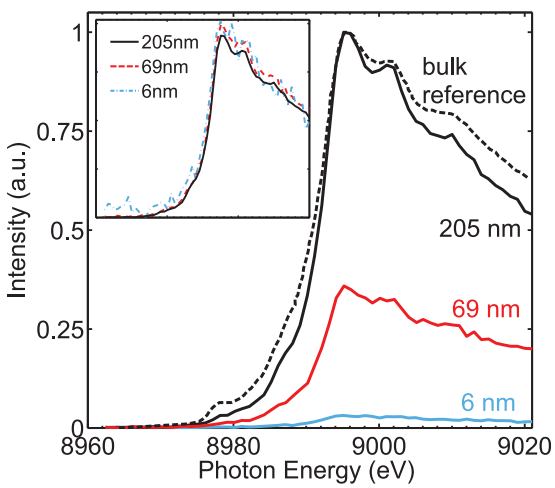

FIG. 2. Normalized Cu K-edge XANES spectra measured on OP Bi-2212 exfoliated crystals on a Si/SiO_2 substrate. The reference bulk data is scaled to the intensity of the 205 nm sample. The inset presents the spectra of the same OP Bi-2212 exfoliated crystals normalized by their thickness.

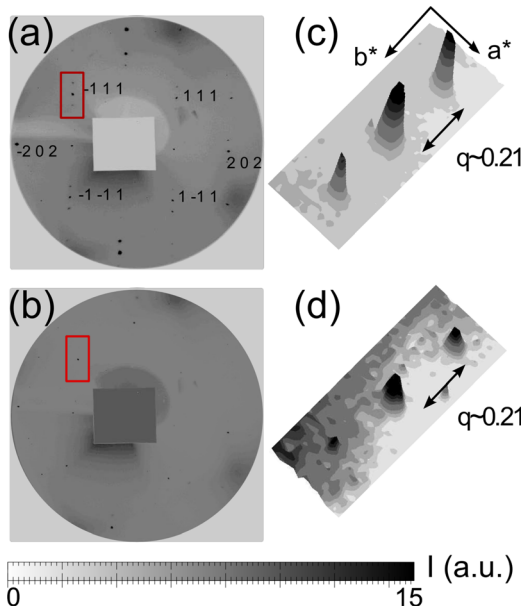

FIG. 3. X-ray diffraction patterns obtained in transmission mode at 15 keV for (a) 69 nm (exposure time of 50 s), (b) 12 nm (exposure time of 100 s). Magnification of the (−111) reflection and the superlattice peaks around it, in the region bounded by the red rectangles: (c) 69 nm crystal, (d) 12 nm. The spacing between the modulation peaks, along the b*−direction, is indicated in units of $2\pi/b$.

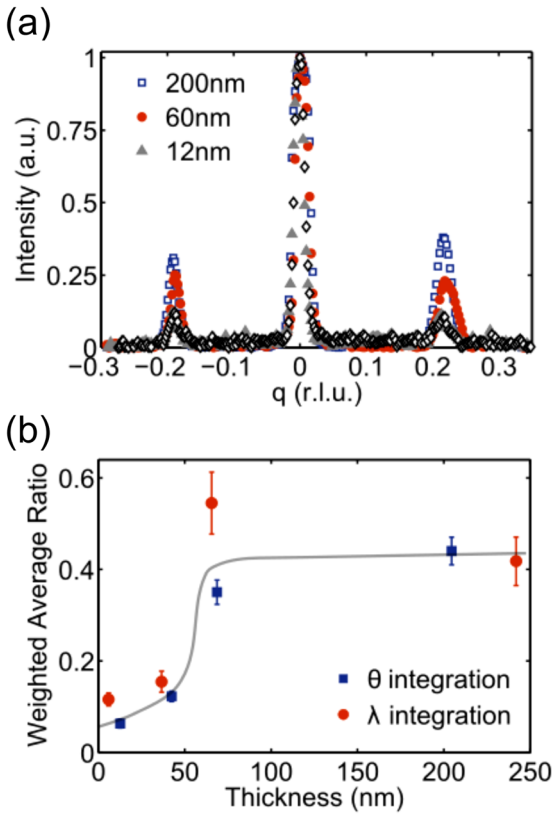

FIG. 4. (a) Integrated intensity around the (−1 1 1) reflection for Bi-2122 nanocrystals of various thicknesses: 12 nm, 40 nm, 60 nm, and 200 nm. The superlattice peaks are observed in the surroundings of the Bragg peaks. (b) The intensity ratio of the modulations as a function of thickness obtained by angle integration (squares) and energy integration (circles). The grey line is a guide to the eye to illustrate the drop in the modulation intensity for thicknesses below ~60 nm.

is not satisfied for the Si substrate. Nevertheless, a four-fold pattern produced by the thermal diffuse scattering of the [100] Si substrate[18] was observed at the edges of the diffraction image.

The Miller indices indicated in Fig. 3(a) correspond to the strongest reflections in the diffraction images and refer to the pseudo-tetragonal unit cell with $a \simeq b \simeq 5.42$ Å and $c \simeq 30.88$ Å. The strongest Bragg peaks can also be found in the image shown in (b), which was obtained for a sample of ~12 nm. The diffraction data indicate that the OP Bi-2212 exfoliated crystals maintain the same crystal structure, from bulk down to thinnest exfoliated nanocrystals, of only 2 unit cells. However, the superstructure modulation is strongly suppressed as the crystal becomes thinner. In Figs. 3(c) and 3(d), one can observe the satellite peaks, which arise from the superstructure of the "4.7 b" modulation[19] and occur at $2\pi/4.7$ b away from the structural Bragg peaks. The satellite peaks are suppressed for the 12 nm crystal. The intensity of the modulation peaks, integrated along the a* direction and normalized to the height of the Bragg peak, is plotted in the b* direction in Fig. 4(a). To quantify the evolution of the modulations, we calculate the ratio between the summed intensity of the superlattice peaks and the central Bragg peak. This ratio was averaged over a set of four symmetry-equivalent Bragg peaks {1 1 1}. The weight of the average is the relative intensity of a Bragg peak in the set. The results are shown in Fig. 4(b). The intensity ratio decreases by a factor of 4 from 200 nm to 12 nm, suggesting that the structural modulation amplitude changes by a factor of two. Moreover, the ratio has a very small decrease until a critical thickness of ~60 nm, below which there is a sudden drop in the modulation intensity. The intensity ratio of the {1 1 1} peaks obtained with the wavelength-integration method also shows a similar trend.

Since the discovery of these structural modulations in bulk crystals, there has been a considerable debate on their origin and the role they play in the mechanism for superconductivity.[19–23] One possible explanation for their origin is the lattice mismatch between the Bi-O rock salt and the Cu-Sr-Ca perovskite layers,[20] which causes a corrugation of the Bi-O layer, leading to a sinusoidal modulation of the Bi atom positions.[21] In view of this hypothesis, removing layers through exfoliation could reduce the interlayer strain and cause a drop in the modulation amplitude, resulting in the suppression of the satellite peak intensity. Another possible origin of the modulations is the extra oxygen ions accommodated in the Bi-O layer to balance the excess charge that arises from the $Bi^{3+} : Sr^{2+}=2.1 : 1.9$ stoichiometry.[19] Some excess oxygens provide holes in the Cu-O plane and modulate the structure,[22] and they can be removed via doping.[23] Similarly, one could expect that the reduced thickness of nanocrystals causes "the loss" of some excess oxygens to the atmosphere thus reducing the intensity of the modulation. Further investigation of the electronic and structural properties of the material is necessary to confirm this scenario. We emphasize that the modulation is suppressed, but it remains present even at low thicknesses of 2–4 unit cells. The correlation length of the "4.7 b" modulations along the c-direction is about 2 nm,[24] much smaller than the samples measured in this study. Therefore, the observed suppression around a thickness of 60 nm is not related to the c-axis correlation

length. We did not observe the "2 a" modulations reported in Refs. 24 and 25. These modulations are 3–4 orders of magnitude weaker than the "4.7 b" modulations we studied and are therefore difficult to detect.

In conclusion, we have performed synchrotron X-ray studies designed to characterize the structure of exfoliated nanocrystals, with thicknesses of a few atomic layers. The study explores the structural properties of $Bi_2Sr_2CaCu_2O_{8+\delta}$ exfoliated nanocrystals, using a combination of X-ray fluorescence mapping, X-ray absorption near edge spectroscopy, and X-ray diffraction with a micro-focused X-ray. The $Bi_2Sr_2CaCu_2O_{8+\delta}$ nanocrystals seem to maintain the same structural and electronic properties as the bulk crystal down to a thickness of 6 nm. The "4.7 b" structural modulations reported in $Bi_2Sr_2CaCu_2O_{8+\delta}$ bulk crystals do not completely disappear down to a thickness of 12 nm but are drastically diminished below a limiting thickness of 60 nm. Preliminary results show that the technique is feasible on Bi_2Se_3 nanocrystals exfoliated on mica or Si/HfO_2 substrate.[14] The techniques we described are generally applicable to structural studies of many nanocrystals exfoliated on various substrates, and could be applied to investigate structure-function relations in these materials.

We would like to acknowledge the assistance of the ECTI Open Research Facility in preparing the samples. The work at the University of Toronto was supported by the Natural Sciences and Engineering Research Council (NSERC) of Canada, Canada Research Chair, and the Canada Foundation for Innovation. The research performed at the Canadian Light Source was supported by NSERC, NRC, CIHR, the Province of Saskatchewan, Western Economic Diversification Canada, and the University of Saskatchewan. We thank Darren Hunter, from the Canadian Light Source, for his assistance with the VESPERS beamline software and equipment.

[1]K. S. Novoselov, D. Jiang, F. Schedin, T. J. Booth, V. V. Khotkevich, S. V. Morozov, and A. K. Geim, Proc. Natl. Acad. Sci. U.S.A. **102**, 10451 (2005).
[2]J. T. Ye, S. Inoue, K. Kobayashi, Y. Kasahara, H. T. Yuan, H. Shimotani, and Y. Iwasa, Nat. Mater. **9**, 125 (2010).
[3]R. V. Gorbachev, I. Riaz, R. Nair, L. Jalil, R. Britnell, B. D. Belle, E. W. Hill, K. S. Novoselov, K. Watanabe, T. Taniguchi, A. K. Geim *et al.*, Small **7**, 465 (2011).
[4]S. Zhao, C. Beekman, L. Sandilands, J. Bashucky, D. Kwok, N. Lee, A. Laforge, S. Cheong, and K. Burch, Appl. Phys. Lett. **98**, 141911 (2011).
[5]K. M. F. Shahil, M. Z. Hossain, D. Teweldebrhan, and A. A. Balandin, Appl. Phys. Lett. **96**, 153103 (2010).
[6]D. Teweldebrhan, V. Goyal, and A. A. Balandin, Nano Lett. **10**, 1209 (2010).
[7]T. Ohta, A. Bostwick, T. Seyller, K. Horn, and E. Rotenberg, Science **313**, 951 (2006).
[8]A. Splendiani, L. Sun, Y. Zhang, T. Li, J. Kim, C.-Y. Chim, G. Galli, and F. Wang, Nano Lett. **10**, 1271 (2010).
[9]C. Lee, H. Yan, L. E. Brus, T. F. Heinz, J. Hone, and S. Ryu, ACS Nano **4**, 2695 (2010).
[10]L. Ren, X. Qi, Y. Liu, G. Hao, Z. Huang, X. Zou, L. Yang, J. Li, and J. Zhong, J. Mater. Chem. **22**, 4921 (2012).
[11]G. E. Ice, J. D. Budai, and J. W. L. Pang, Science **334**, 1234 (2011).
[12]I. McNulty, B. Lai, J. Maser, D. J. Paterson, P. Evans, S. M. Heald, G. E. Ice, E. D. Isaacs, M. L. Rivers, and S. R. Sutton, Synchrotron Radiat. News **16**, 34 (2003).
[13]J. L. Jordan-Sweet, IBM J. Res. Dev. **44**, 457 (2000).
[14]See supplementary material at http://dx.doi.org/10.1063/1.4768234 for additional information on the structural study of $Bi_2Sr_2CaCu_2O_{8+\delta}$ nanocrystals and preliminary data on Bi_2Se_3 exfoliated nanocrystals.
[15]R. Feng, A. Gerson, G. Ice, R. Reininger, B. Yates, and S. McIntyre, AIP Conf. Proc. **879**, 872 (2007).
[16]A. P. Hammersley, S. O. Svensson, A. Thompson, H. Graafsma, Å. Kvick, and J. P. Moy, Rev. Sci. Instrum. **66**, 2729 (1995).
[17]N. L. Saini, A. Lanzara, A. Bianconi, and H. Oyanagi, Phys. Rev. B **58**, 11768 (1998).
[18]M. Holt, Z. Wu, H. Hong, P. Zschack, P. Jemian, J. Tischler, H. Chen, and T.-C. Chiang, Phys. Rev. Lett. **83**, 3317 (1999).
[19]V. Petricek, Y. Gao, P. Lee, and P. Coppens, Phys. Rev. B **42**, 387 (1990).
[20]X. B. Kan and S. C. Moss, Acta Crystallogr., Sect. B: Struct. Sci. **48**, 122 (1992).
[21]Y. Le Page, W. R. McKinnon, J.-M. Tarascon, and P. Barboux, Phys. Rev. B **40**, 6810 (1989).
[22]H. Eisaki, N. Kaneko, D. L. Feng, A. Damascelli, P. K. Mang, K. M. Shen, Z.-X. Shen, and M. Greven, Phys. Rev. B **69**, 064512 (2004).
[23]N. Fukushima, H. Niu, S. Nakamura, S. Takeno, M. Hayashi, and K. Ando, Physica C **159**, 777 (1989).
[24]J. P. Castellan, B. D. Gaulin, H. A. Dabkowska, A. Nabialek, G. Gu, X. Liu, and Z. Islam, Phys. Rev. B **73**, 174505 (2006).
[25]M. Izquierdo, S. Megtert, J. P. Albouy, J. Avila, M. A. Valbuena, G. Gu, J. S. Abell, G. Yang, M. C. Asensio, and R. Comes, Phys. Rev. B **74**, 054512 (2006).